# Gait Phase Recognition based on SVM Classifier Optimized by Particle Swarm Optimization with Local Fast Searching Strategy

Fenggang Liu

Abstract—This paper presents an intelligent wearable sensor data acquisition system used to collect the plantar pressures and joint angles for the classification of human gait patterns. The whole system is designed and equipped with two force-sensitive resistors (FSRs) and three inertial measurement units (IMUs) for each leg. The sensor data are transmitted via Bluetooth to a host computer for storage. The support vector machine (SVM) algorithm is employed to identify the sensor data into the specific gait patterns. To enhance the performance for SVM classifying the gait patterns, a local fast search (LFS) strategy is integrated into the classic particle swarm optimization (PSO) algorithm for parameter optimization. The LFS strategy integrates three key mechanisms, including in nonlinear adaptive inertia weight, performance driven learning factors, and diversity preserving mutation. For comparative analysis, three distinct algorithms were developed for gait phase recognition, such as SMV, PSO-SVM and LFS-PSO-SVM. Experimental results show that the presented LFS-PSO-SVM approach exhibits superior performance, and achieves the highest accuracy in gait phase identification. The study validates the robustness of the motion data acquired by the smart collection system and proves the effectiveness of the proposed algorithm in gait analysis applications.

Index Terms—FSR, IMU, SVM, Local fast search, PSO.

#### I. INTRODUCTION

Gait analysis is a useful tool in computer vision and humanized robots that focus on classifying the different body motion patterns, such as swing and stance [1-2]. It has shown significantly important values due to its ability to aid various applications, including human action perception, activity analysis, and control implementation [3]. The study of gait analysis can contribute to advancing the robots' cognitive abilities, and enabling them to infer movement patterns and contextual information. Moreover, it can enhance our understanding of human dynamics in different settings, such as industrial automation for robot operation monitoring, smart manufacturing for predictive maintenance, healthcare informatics for patient health assessment, and traffic management for traffic signal optimization [4-6].

Many researchers had showed their interests in gait phase recognition for their abilities to handle complex dynamic scenarios. The existing techniques include in artificial neural

Manuscript received February 19, 2025; revised September 11, 2025. Fenggang Liu is an Associate Professor at the School of Artificial Intelligence, Wuchang University of Technology, Wuhan, 430221, China. (corresponding author to provide phone: +86 15377677072; e-mail: fg liu1314@163.com).

networks [7], bidirectional long short-term memory and deep neural networks [8], random forests [9], convolutional neural networks (CNN) [10], multi-task recurrent neural networks [11], and support vector machines (SVM) [12-14]. Nahian Rifaat et al presented a new deep neural network architecture to realize accurate gait recognition with inertial sensors [15]. The gait data are from the OU-ISIR and whuGAIT, and the features are extracted by CNN. The experimental results showed that the proposed methods can be used for biometric systems to benefit the human being. Guo et al introduced a transferable multi-modal fusion to predict the knee angles and gait phases by fusing many signals [16]. The experiments demonstrated that the proposed method can gain a root mean square error of  $0.090 \pm 0.022$  s in knee angle prediction and a precision of 83.7  $\pm$  7.7% in gait phase prediction. Bauman and Brandon developed a supervised multi-class classifier to identify the gait phases through inertial measurement units (IMU) data from the thigh and shank [17]. The aim of this method was to control the lower limb exoskeleton, and this proposed classifier gained an accuracy of 97.1% for the lower limb exoskeleton. Wu et al combined the SVM and finite state machine (FSM) to classify the gait phases [18]. The SVM is improved by introducing the K-means clustering to reduce the model size, and the FSM is used to validate the prediction and correct the wrong detection. The experimental results showed that this approach achieved an accuracy of 91.51% in gait phase recognition. The success of these studies highlights the importance of innovative approaches to make gait phase recognition more practical and efficient.

On the other side, the optimization methods are usually utilized to optimize the parameters for these classifiers. Yu et al. used the particle swarm optimization (PSO) to search the best SVM model parameters for higher accuracy in gait phase recognition [19]. Moodi et al. proposed a smart self-adaptive learning PSO to optimize the SVM model [20]. Cui et al proposed an adaptive PSO-SVM to addresses the premature convergence issue during the gait pattern recognition process [21]. The optimization methods could help find the best parameters for classifiers, which leads to higher performance.

To identify the gait phases, this paper designed a wearable system to collect the force and angle data. The measured data are classified as six gait patterns labeled by detection rules. The SVM algorithm is selected to identify these gait patterns. To enhance the performance in gait phase identification, this study integrates the PSO with local fast search (LFS) strategy to optimize the SVM parameters. The LFS strategy integrates three key mechanisms, including in nonlinear adaptive inertia weight, performance driven learning factors, and diversity

preserving mutation, which aiming to improve the global search capability and convergence speed for PSO. The experimental results show that the proposed LFS-PSO-SVM gains a high recognition accuracy for gait phase recognition.

#### II. MATERIALS AND METHOD

#### A. Design of Intelligent Shoe

As pictured in Figure 1, an intelligent shoe is designed and mounted with two force sensitive resistors (FSR) and three IMUs. The FSRs are separately located in the ball and heel parts in one foot, while the IMUs are bound on the lower limbs of tight, shank and foot. The FSR is used to measure the ground contact forces (GCF), while the IMU is to monitor the joint rotary angle. The sensor data are collected by a signal acquisition circuit board of STM32 processor powered by a rechargeable 3.3V battery. The A/D converter and Bluetooth module are integrated inside the STM32 processor. The sensor data are digitized by the A/D converter and transferred by the Bluetooth module into personal computer. The detailed diagrams are depicted in Figure 2, and the sampling frequency is 100 Hz.

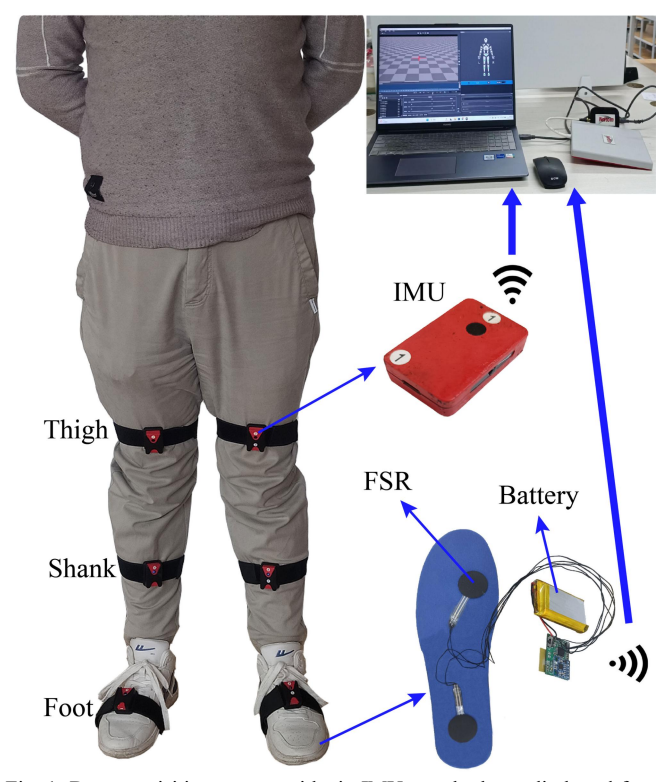


Fig. 1. Data acquisition system with six IMUs on the lower limb and four FSRs inside the shoe.

#### B. Segmentation and Labeling of Gait Patterns

The stance and swing phases are the two main phases in a typical human walking which is periodic and cyclic. The foot is touching the ground all the time during the stance phase, while the entire foot is leaving the ground during the swing phase. Additionally, the stance phases can be subdivided into the heel striking (HS), full stance (FS) and heel off (HO), while the swing phases can also be subdivided into pre-swing (PS), middle swing (MS) and terminal swing (TS). As shown in Figure 3, a complete gait cycle consists of the above six

patterns. These phases occur sequentially one after the other, and each phase lasts for a certain duration.

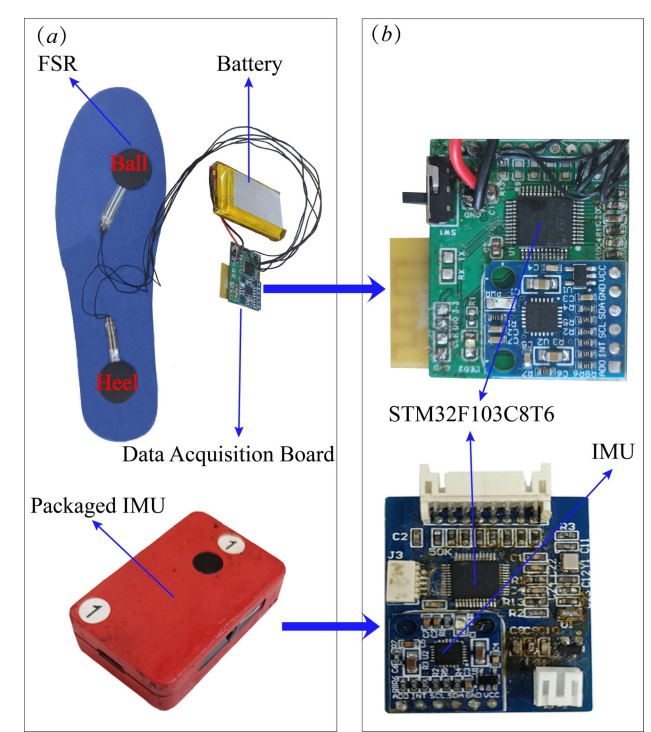


Fig. 2. Sensor data collected by the STM32 processor: (a) The FSRs and IMU module, (b) The physical diagram of STM32 and internal structure of IMU module.

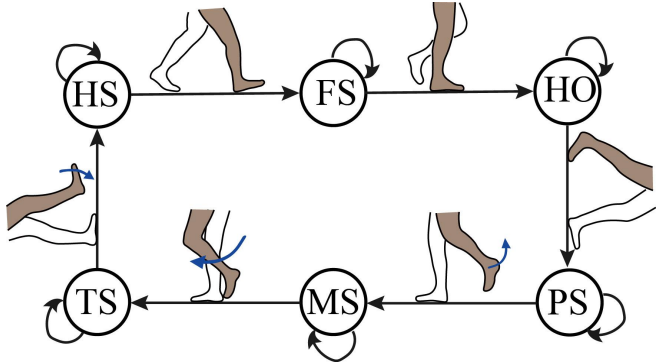


Fig. 3. Six phases in a gait cycle.

The stance phase begins when the heel touches the ground and ends when the ball is ready to leave the ground. The swing phase starts when the foot totally leaves the ground and ends when the heel is ready to contact the ground again. The state of touching or leaving the ground can be judged by comparing the GCF with a threshold. If the GCF is larger than the threshold, the state is on-ground. Otherwise, the state is off-ground. The gait pattern is designated as HS when the heel is determined to be on-ground state and the ball is off-ground state. The gait pattern is labeled as FS when the heel and ball are both determined to be on-ground state. The gait pattern is designated as HO when the heel is determined to be off-ground state and the ball is on-ground state. The gait pattern is designated as swing when both the heel and the ball are determined to be off-ground state.

Twenty one healthy subjects volunteered to participate in our experiments. They were asked to wear the shoes to walk on treadmill for one minutes. As illustrated in Figure 4, the force and angle data are obtained and filtered by the Butterworth filter with the cut-off frequency of 10 Hz. The

data are converted into specific gait patterns by following the above rules. The stance and its subdivision can be determined through setting a threshold and corresponding rules. The subdivision of swing phase can be quantified by the ankle joint angle. When the entire foot is judged as off-ground state and the ankle joint angle decreases, this process is determined as PS. Then, the ankle joint angle decreases to its negative maximum and starts to increase, this process is MS. Finally, the ankle joint angle increases to its negative minimum and begins to decrease, this process is TS.

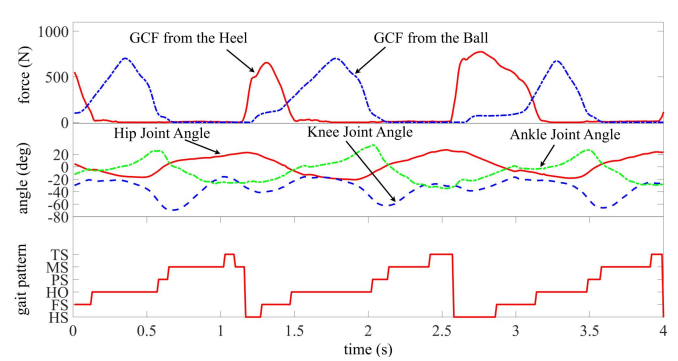


Fig. 4. Data of forces and angles and gait phase division through the detection rules.

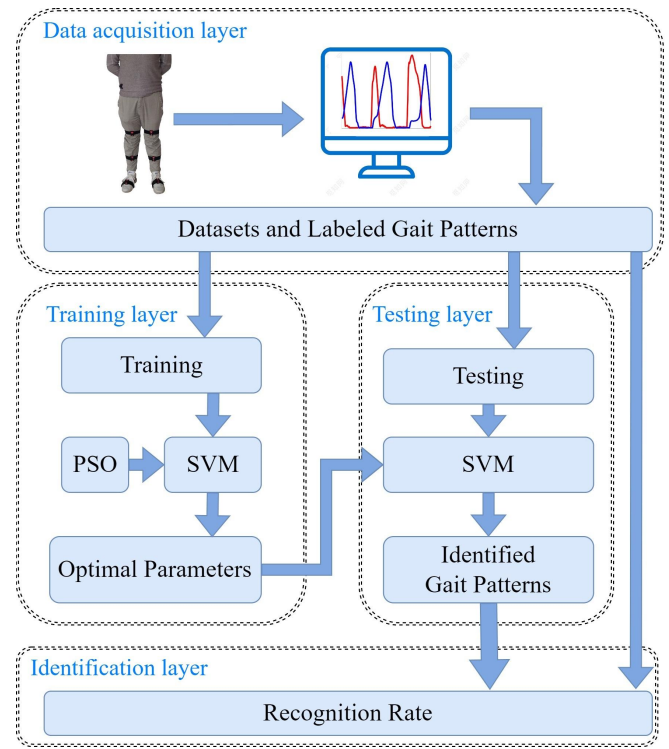


Fig. 5. Flow diagram of PSO optimizing SVM.

## III. GAIT PATTERN RECOGNITION THROUGH SUPPORT VECTOR MACHINE

In this paper, the SVM classifier is selected to recognize the gait patterns. The collected data are divided into training and testing parts. The training data possesses 70% of the whole data, while the remaining 30% are the testing data. The SVM model was trained through the training data, and its parameters are optimized by the PSO algorithm. The gait patterns are then determined by feeding the testing data into the SVM model with the optimal parameters. Lastly, by

comparing the identified results with the labeled ones, the recognition rate can be calculated. The flow diagram of PSO optimizing SVM is depicted in Figure 5.

#### A. Support Vector Machine

The basic idea of SVM classifier is to utilize a nonlinear transformation to translate the vector (i.e., the sensor data) to a high-dimensional space, and then select a kernel function to solve the optimal linear classification surface in the new high-dimensional space. It is a great challenge to compute the feature spaces mapping the low-dimensional input space to the high-dimensional feature space due to the rapid rise of the spatial dimension. The k-class optimization problem can be characterized that it is tackled by specifying the relaxation variable  $\xi = (\xi_1, \xi_2, ..., \xi_m)$  and training simultaneously with a single objective function.

$$\begin{cases}
\min \frac{\|w\|^2}{2} + C \sum_{i=1}^m \xi_i \\
s.t. \begin{cases}
yi, (w \cdot x_i + b)^a > 1 - \xi_i \\
\xi_i \ge 0
\end{cases} 
\end{cases}$$
(1)

where b is the bias, w is the vector of weights, m is the number of slack variables, and C is a positive constant. a is a constant coefficient. This problem is translated into the input space for computation by the optimum classification surface SVM, which use the kernel functions to yield the decision function.

$$f(x) = \operatorname{sgn}\left\{ \sum_{i=1}^{n} y_i a_i^* K(x_i \cdot x) + b^* \right\}$$
 (2)

where  $a_i$  is the Lagrange multiplier. There are two training sample sets.

$$D = \{(x_i, y_i) |_{i=1}^n, x_i \in X \subseteq R^n, y_i \in Y \subseteq \{-1, 1\}, \}$$
 (3)

where n is the training sample vector's dimension, while -1 and 1 stand for the category numbers. The distance between any point on the two samples and the classification surface is higher than or equal to 1. The ideal classification surface wx+b=0 is found in order to accurately categorize the two patterns. The SVM uses a nonlinear transformation that depends on the kernel function to accomplish complex operations in low dimensional space and determine the best classification surface in high dimensional space.

#### B. Particle Swarm Optimization (PSO) Algorithm

The PSO is an algorithm for iterative optimization, which can handle a wide range of optimization issues. The particle position, velocity, and fitness are their primary attributes. The aim is to find the maximum or minimum value for the fitness, and the global optimal solution is found by adjusting the particle's position and velocity during the search process. In each iteration, the particles' position and velocity would be updated through the following equation.

$$\begin{cases} v_{i,j}(t+1) = w_0 v_{i,j}(t) + c_1 r_1(p_{i,j} - x_{i,j}(t)) + c_2 r_2(p_{g,j} - x_{i,j}(t)) \\ x_{i,j}(t+1) = x_{i,j}(t) + v_{i,j}(t) \end{cases}$$

where  $w_0$  is the inertia weight. The flying velocity is indicated as  $v_{i,j}(t+1)$ , the position is written as  $x_{i,j}(t+1)$ , the individual optimal solution for the *i-th* particle is  $p_{i,j}$ , and the global optimal solution is  $p_{g,j}$ . The individual and global extreme positions are represented by the factors  $c_1$  and  $c_2$ . The random numbers distributed in the interval [0,1] are denoted by  $r_1$  and  $r_2$ .

#### C. Local Fast Search-Particle Swarm Optimization

With the usage of an adjustable search step size, the local fast search (LFS) strategy is presented to increase the searching efficiency of PSO. While the enormous step size of the PSO algorithm can effectively search on a broad scale, it will not be able to search for the global optimal solution when used to high-dimensional extremum issues. In the meantime, the global search accuracy for the best solution will also be greatly impacted by the step size decay rate. Therefore, an LFS strategy is created to swiftly search the possible global optimal solution area such that the algorithm can still jump out of the local optimum, minimize the effect of step size on parameter optimization, and improve the search accuracy. This proposed LFS strategy consists of three key mechanisms, such as nonlinear performance driven learning factors, adaptive inertia weight and diversity preserving mutation, which are described detailedly in the following.

#### (1) Performance driven learning factors

The primary goal of the LFS strategy is to determine a local search step size, and lock the step size in the current iteration. The adaptive attenuation of the step size is finished in the LFS, and the local search step size is unique to the LFS. Therefore, in order to improve the search results for PSO, a new variable  $\delta$  is presented.

$$\delta(t) = \lambda^{\frac{a_0}{b_0 + \gamma t / m}} \delta(t - 1) \tag{5}$$

where  $a_0$ ,  $b_0$ , and  $\gamma$  are constants and their sizes influence the decay rate of  $\delta$ . Meanwhile, t is the number of LFS iteration, while m is the maximum number of LFS iteration, which must be chosen such that search speed and accuracy are balanced. The range of  $\lambda$  is given between 0 and 1. The initial value  $\delta(0)$  is an independent variable that is independently attenuated. The Equation (5) in the local quick search section also has to be modified in the manner described below.

$$\begin{cases} v_{i,j}(t+1) = w_0 v_{i,j}(t) + c_1 r_1(p_{i,j} - x_{i,j}(t)) + c_2 r_2(p_{g,j} - x_{i,j}(t)) \\ x_{i,j}(t+1) = x_{i,j}(t) + \delta(t) v_{i,j}(t) \end{cases}$$
(6)

The inclusion of a weighting strategy with randomly selecting  $w_0$  values makes the effect of the particles' historical speed on the current speed random.

#### (2) Nonlinear adaptive inertia weight

First, if the best point is approached early in the evolution, the random w may produce a relatively small value of  $w_0$ , which would speed up the algorithm's convergence. Alternatively, if the best point cannot be found at the beginning of the algorithm, the linear decreasing of  $w_0$  makes the algorithm converge less than the best point, and the random generation of  $w_0$  can overcome this limitation. The weight would eventually drop as the fitness progressively declined to haste the algorithm's convergence. The random weigh can be described as follow.

$$\begin{cases} w_0(t) = \left[ w_{\text{max}} - (w_{\text{max}} - w_{\text{min}}) \left( \frac{t}{T_{\text{max}}} \right)^2 \right] \cdot (1 + 0.5(1 - D_t)) \\ D_t = \frac{1}{N} \sum_{i=1}^{N} std(x_t^i) \end{cases}$$
 (7)

where  $D_t$  is the population diversity measured by position variance, and  $x_t^i$  denotes the *i-th* dimension coordinates of all particles at iteration t. The quadratic term accelerates early exploration, while the diversity term  $D_t$  dynamically balances exploitation when population converges.

#### (3) Diversity preserving mutation.

Meanwhile, the  $c_1$  and  $c_2$  are updated through dynamic adjustment mechanism, which can be described in the following.

$$\begin{cases} c_{1}(t) = c_{10} \cdot (1 + 0.1 \cdot \frac{\sum_{i=1}^{N} S_{i}^{t}}{N}) \\ c_{2}(t) = c_{20} \cdot (1 - 0.1 \cdot \frac{\sum_{i=1}^{N} S_{i}^{t}}{N}) \end{cases}$$
(8)

where  $c_{10}$  and  $c_{20}$  are the initial values for  $c_1$  and  $c_2$ .  $x_t^i$  indicates the stagnation status, which can be written in the following.

$$S_i^t = \begin{cases} 1, & f(x_i^t) = f(pbest_i^t) \\ 0, & others \end{cases}$$
 (9)

where  $f(\cdot)$  is the function to compute the fitness. This adaptation method increases the cognitive learning ability for stagnant particles in order to enhance the social learning for progressing particles.

The proposed LFS strategy implements the enhancements sequentially in each iteration for PSO. The first step is to calculate diversity metric  $D_t$ . The second step 2 is to update the  $w_0$ ,  $c_1$  and  $c_2$ . The third step is to perform the velocity and position updating. The last step is to update the local and global best positions. The synergistic integration establishes an adaptive balance between global exploration and local exploitation throughout the optimization process.

#### D. LFS-PSO-SVM model

The parameters selection is extremely important for SVM model in gait phase recognition. The parameters C and  $\gamma$  in SVM model are optimized by the proposed LFS-PSO, and

the whole structure is established in Figure 6. The flow of LFS-PSO optimizing SVM are described in below. The first step is to initialize the particles (i.e., C and  $\gamma$ ), population and set the algorithm parameters. The second step is to update the velocity and particle according to the LFS strategy. The third step is to run the SMV with new particles. The best particles are gained until the iteration reaches its maximum value.

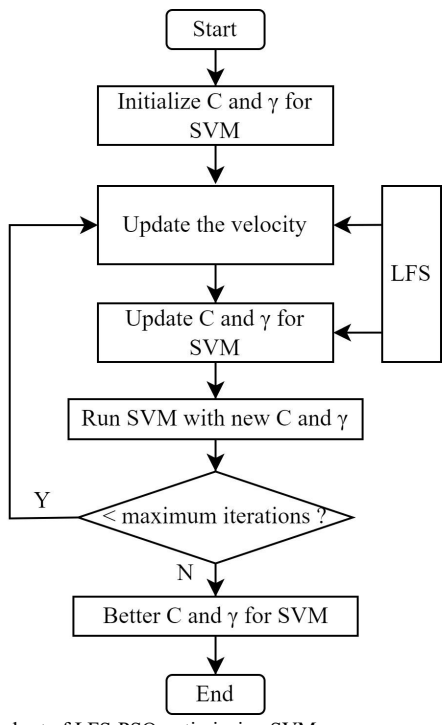


Fig. 6. Flow chart of LFS-PSO optimizaing SVM

#### IV. RESULTS

#### A. Selection of SVM parameters

The penalty factor C and kernel function parameter  $\gamma$  for the SVM model are determined through the empirical technique. By loading C=2 and  $\gamma$  = 1 into the SVM model, the training data are used to find the best hyperplane for classification. Then, the testing data are input into the trained hyperplane and identified as specific gait patterns. All kernel functions are tested to obtain the recognition accuracy, and Table I displays the results. It can be found that the SVM model with the polynomial or RBF kernel functions obtained higher recognition accuracies compared with the others. The RBF kernel function is finally chosen because it performs better in response time than the polynomial kernel function.

TABLE I
RECOGNITION RESULTS OF DIFFERENT KERNEL FUNCTION

RECOGNITION RESCETS OF BITTERENT RESCREET ONCTION						
Kenel Function	Parameter	Accuracy	Response time			
Polynomial	$C=2, \gamma=1$	94.73%	1.5 s			
RBF	$C=2, \gamma=1$	94.39%	0.5 s			
Linear	$C=2, \gamma=1$	90.90%	0.5 s			
Sigmoid	$C=2, \gamma=1$	58.91%	1 s			

The PSO algorithm is used to optimize the parameters C and  $\gamma$ , and the particle dimension is set to be 2. In order to gain accurate results and train the SVM fast, the population size is given to be 20, the maximum iteration number is assigned to be 100, and the local (i.e.,  $c_1$ ) and global (i.e.,  $c_2$ ) acceleration factors are set to be 1.5 and 1.7, respectively.

For the proposed LFS-PSO,  $c_{10}$  and  $c_{20}$  are both 2,  $w_{max}$  is set to be 0.9, and  $w_{min}$  is given to be 0.4. Moreover,  $a_0$  and  $b_0$  in Equation (5) are both set to be 0.2,  $\gamma$  is 0.8, and m is the maximum iteration number 100.

As shown in Figure 7, the proposed LFS-PSO can achieve higher fitness than the original PSO in gait phase recognition. Moreover, the LFS-PSO costs about 30 times to realize stable fitness, while the PSO needs 47 times. The results shows that the LFS-PSO can enhance the search speed and achieve higher performance in gait phase recognition.

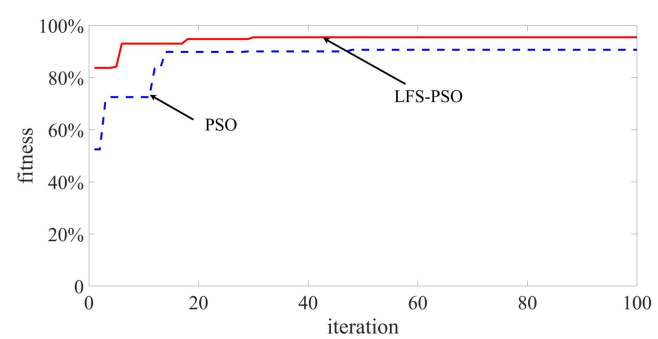


Fig. 7. Fitness for two methods.

#### B. Result analysis of gait phase recognition

As shown in Figure 8, the collected data are transformed into specific gait patterns according to the above-mentioned labeling rules. Then, the data are classified as specific gait patterns based on the SVM model. It can be clearly found that the identified gait patterns are recognized as the correct ones at most of the time. However, there still exist some wrong identifications. To overcome this problem, the optimization methods are used to find the best parameters for SVM model to gain a higher accuracy.

TABLE II
GAIT PHASE RECOGNITION RESULTS FOR ALL SUBJECTS

	SVM PSO-SVM LFS-PSO-SVM						
		M	PSO-SVM		LFS-PSO-SVM		
No.	Precisio n	Recall	Precisi on	Recall	Precisio n	Recall	
1	89.79%	88.26%	92.67%	92.96%	93.68%	94.52%	
2	89.43%	90.65%	94.59%	92.95%	93.91%	94.53%	
3	89.40%	91.89%	94.92%	92.35%	94.74%	95.45%	
4	91.60%	92.67%	94.59%	94.60%	94.24%	95.38%	
5	90.73%	88.64%	93.80%	92.47%	96.69%	94.93%	
6	90.64%	90.84%	94.18%	91.44%	94.72%	94.13%	
7	89.43%	90.34%	93.18%	94.12%	93.73%	95.43%	
8	91.55%	88.05%	94.97%	92.55%	96.61%	94.59%	
9	90.86%	89.68%	92.75%	91.96%	96.91%	94.05%	
10	90.05%	88.81%	94.74%	92.61%	94.75%	95.81%	
11	90.53%	91.97%	92.73%	91.38%	93.44%	95.62%	
12	90.20%	89.55%	93.47%	91.52%	94.03%	94.65%	
13	89.22%	90.64%	94.50%	94.76%	94.63%	94.86%	
14	89.71%	88.82%	95.12%	94.82%	95.37%	94.76%	
15	89.37%	91.11%	92.32%	93.30%	94.04%	93.62%	
16	89.55%	89.31%	95.71%	91.23%	95.41%	93.90%	
17	89.71%	91.27%	95.10%	91.93%	95.84%	94.41%	
18	90.25%	91.44%	93.94%	92.41%	93.88%	93.69%	
19	89.14%	91.74%	93.74%	94.28%	93.46%	95.53%	
20	91.70%	90.25%	93.78%	91.06%	94.18%	93.58%	
21	91.83%	88.41%	93.22%	91.17%	94.27%	93.67%	
avg	90.22%	90.21%	94.01%	92.66%	94.69%	94.62%	

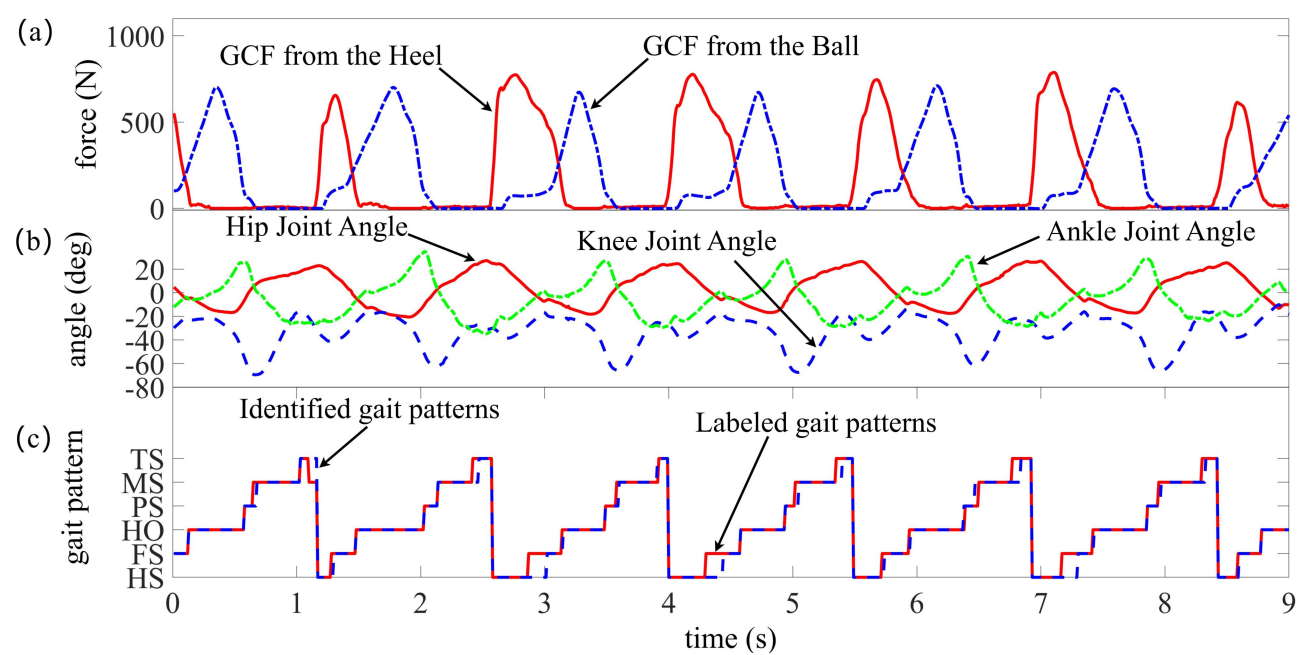


Fig. 8. Results of gait pattern recognition through SVM model.

Twenty-one subjects volunteered to participate in our experiments, and the gait phase recognition results for them are listed in Table II. A large number of experiments can explain the problem. The original SVM gains an average precision of 90.22% and an average recall of 90.21%. The PSO-SVM realizes an average precision of 94.01% and an average recall of 92.66%. The proposed LSF-PSO-SVM acquires an average precision of 94.69% and an average recall of 94.62%. The experiments indicate that the proposed methods obtain the highest results in terms of precision and recall.

The results of SVM, PSO-SVM, and LFS-PSO-SVM models are pictured in Figure 9, Figure 10 and Figure 11 in the forms of confusion matrix. The proposed LFS-PSO-SVM gains the highest accuracy in clarifying the gait phases of HS, PS, MS and TS, while the PSO-SVM achieves the best in identification of HO and PS phases. The quantitative results are listed In Table III. In terms of overall performance, the LFS-PSO-SVM model exhibits the highest average performance, and achieve an average recall of 95.11% and an average precision of 94.31%, surpassing both the SVM and PSO-SVM models. The PSO-SVM model also gain an average recall 94.04% and precision of 94.62% compared to the average recall 91.14% and precision 91.72% from the original SVM.



Fig. 9. Classification confusion matrix of the SVM model.

HS	94.6%	1.9%	0.0%	0.0%	0.0%	3.5%	
	6189	124	0	0	0	226	
(Labeled) H O S	2.6% 124	95.0% 4520	2.4% 113	0.0% 0	0.0% 0	0.0%	
S (Lab	0.0% 0	0.9% 112	98.0% 12546	1.1% 138	0.0% 0	0.0%	
ut Class	0.0%	0.0%	3.4%	92.1%	4.5%	0.0%	
Sd	0	0	89	2422	118		
Output	0.0%	0.0%	0.0%	1.1%	97.4%	1.4%	
	0	0	0	98	8446	124	
TS	5.7%	0.0%	0.0%	0.0%	3.9%	90.4%	
	138	0	0	0	93	2180	
	HS FS HO PS MS TS Target Class (Identified)						

Fig. 10. Classification confusion matrix of the PSO-SVM model.



Fig. 11. Classification confusion matrix of the LFS-PSO-SVM model.

Among all gait phases, the HO phase consistently realizes the highest classification performance across all models, and the LFS-PSO-SVM model achieves a recall of 97.93% and a precision of 98.45% in HO phase classification. Conversely, the TS phase gains the worst results, and the LFS-PSO-SVM model achieve a recall of 91.79% and a precision of 86.68%. Despite notable improvements over the original SVM, the TS phase continues to exhibit the lowest performance metrics, indicating room for further optimization.

We compared our work with other studies in gait phase recognition as shown in Table IV. The References [19] and [22] are both to classify four types of gait patterns. The Reference [22] gained a higher recall than the proposed

method in this paper, but reached a lower precision. The Reference [23] is to identify six types of gait patterns which are different from the ones in this paper. Moreover, the Reference [23] acquired a higher recall compared to the proposed method in this paper, but reached a lower precision. The results indicate that the presented approach gains the highest precision and shows convincing competitiveness in the field of gait phase classification.

TABLE III
CLASSIFICATION CONFUSION MATRIX OF THE THREE MODELS.

	SVM		PSO-SVM		LFS-PSO-SVM	
Gait Recall	Dogg 11	Precisio	Recall	Precisio	Recall	Precisio
	Recair	n		n		n
HS	91.37%	93.98%	94.65%	95.94%	94.8%	95.93%
FS	91.15%	91.55%	95.02%	95.04%	94.62%	95.66%
НО	97.19%	97.13%	98.05%	98.42%	97.93%	98.45%
PS	88.02%	87.52%	92.13%	91.12%	93.61%	90.98%
MS	96.34%	96.35%	97.44%	97.56%	97.89%	98.13%
TS	86.27%	80.31%	90.42%	86.17%	91.79%	86.68%

TABLE IV COMPARISON WITH OTHER STUDIES.

References	Classifier	Gait Number	Recall	Precision
K. Liu [22]	LSTM-CNN	Four	95.29%	95.03%
F. L. Yu [23]	CNN-GRU	Six	94.51%	93.22%
L. Yu [19]	PSO-SVM	Four	94.16%	95.06%
this paper	LFS-PSO-SVM	Six	94.30%	95.10%

#### V. DISCUSSION

The proposed LFS-PSO-SVM model shows significant advancements in gait phase classification. This model achieves the highest average precision, which could indicate its robustness and reliability in gait phase classification tasks. This model demonstrates its ability to handle complex gait patterns such as HS, PS and TS, and exhibits balanced performance across all phases exceeding 90% in terms of recall and precision. This balance is critical for real-world applications where both false positives and false negatives must be minimized.

Future work could focus on extracting more useful features, particularly for the TS phase. Incorporating temporal, spatial, and kinematic features may help improve the classification accuracy. Combining LFS-PSO with deep learning methods could leverage the strengths of both traditional machine learning and deep learning to improve the performance for complex phase like TS.

#### VI. CONCLUSION

This paper introduced a wearable sensor collection system which measured the pressure and angle information for gait pattern classification. After data acquisition and preprocess, the data are input into the SVM model to recognize the gait patterns. The LFS strategy is integrated with the PSO to optimize the SVM parameters for higher performance. The experimental results showed that the LFS-PSO-SVM model gains a significant advancement in gait phase classification, and achieves superior performance and robustness compared to traditional SVM and PSO-SVM approaches. Specifically, the average precision increases from 90.22% to 94.69%, while the average recall improves from 90.21% to 94.62%.

However, challenges such as the classification of TS phase highlight areas for future improvement. By addressing these limitations through enhanced feature engineering, advanced optimization techniques, and hybrid model architectures, the LFS-PSO-SVM framework can be further refined to achieve even greater accuracy in real-world scenarios.

#### REFERENCES

- [1] H. T. T. Vu, D. Dong, H. L. Cao, T. Verstraten, D. Lefeber, B. Vanderborght, and J. Geeroms, "A Review of Gait Phase Detection Algorithms for Lower Limb Prostheses," *Sensors*, vol. 20, no. 14, pp. 3972, 2020.
- [2] M. H. Khan, M. S. Farid, and M. Grzegorzek, "A Comprehensive Study on Codebook-Based Feature Fusion for Gait Recognition," *Inf. Fusion*, vol. 92, pp. 216-230, 2022.
- [3] J. Song, A. Zhu, Y. Tu, H. Mao, and X. Zhang, "Adaptive Neural Fuzzy Reasoning Method for Recognizing Human Movement Gait Phase," *Robotics and Autonomous Systems*, vol. 153, p. 104087, 2022.
- [4] Y. J. Castano-Pino, M. C. Gonzalez, V. Quintana-Pena, J. Valderrama, B. Munoz, J. Orozco, and A. Navarro, "Automatic Gait Phases Detection in Parkinson Disease: A Comparative Study," *Annu. Int. Conf. IEEE Eng. Med. Biol. Soc.*, pp. 798-802, 2020.
- [5] M. Milovic, G. Farías, S. Fingerhuth, F. Pizarro, G. Hermosilla, and D. Yunge, "Detection of Human Gait Phases Using Textile Pressure Sensors: A Low Cost and Pervasive Approach," *Sensors*, vol. 22, no. 8, p. 2825, 2022.
- [6] E. Alijanpour and D. M. Russell, "Gait Phase Normalization Resolves the Problem of Different Phases Being Compared in Gait Cycle Normalization," *J. Biomech.*, vol. 173, p. 112253, 2024.
- [7] S.-H. Yan et al., "Gait Phase Detection by Using a Portable System and Artificial Neural Network," *Medicine in Novel Technology and Devices*, vol. 12, p. 100092, 2021.
- [8] Z. Zhang et al., "Gait Phase Recognition of Lower Limb Exoskeleton System Based on the Integrated Network Model," Biomedical Signal Processing and Control, vol. 76, p. 103693, 2022.
- [9] M. Lee, J.-H. Lee, and D.-H. Kim, "Gender Recognition Using Optimal Gait Feature Based on Recursive Feature Elimination in Normal Walking," *Expert Systems with Applications*, vol. 189, p. 116040, 2022.
- [10] U. Martinez-Hernandez, M. I. Awad, and A. A. Dehghani-Sanij, "Learning Architecture for the Recognition of Walking and Prediction of Gait Period Using Wearable Sensors," *Neurocomputing*, vol. 470, pp. 1-10, 2022.
- [11] C. F. Martindale et al., "Wearables-Based Multi-Task Gait and Activity Segmentation Using Recurrent Neural Networks," *Neurocomputing*, vol. 432, pp. 250-261, 2021.
- [12] W. Teufl et al., "Automated Detection and Explainability of Pathological Gait Patterns Using a One-Class Support Vector Machine Trained on Inertial Measurement Unit Based Gait Data," *Clinical Biomechanics*, vol. 89, p. 105452, 2021.
- [13] B. Vidya and P. Sasikumar, "Gait Based Parkinson's Disease Diagnosis and Severity Rating Using Multi-Class Support Vector Machine," Applied Soft Computing, vol. 113, p. 107939, 2021.
- [14] J. Zheng et al., "PSO-SVM-Based Gait Phase Classification During Human Walking on Unstructured Terrains: Application in Lower-Limb Exoskeleton," Proc. Inst. Mech. Eng. Part C: J. Mech. Eng. Sci., vol. 233, no. 19-20, pp. 7144-7154, 2019.
- [15] N. Rifaat, U. K. Ghosh, and A. Sayeed, "Accurate Gait Recognition with Inertial Sensors Using a New FCN-BiLSTM Architecture," *Computers and Electrical Engineering*, vol. 104, p. 108428, 2022.
- [16] Z. Guo, H. Zheng, H. Wu, J. Zhang, G. Zhou, and J. Long, "Transferable Multi-Modal Fusion in Knee Angles and Gait Phases for Their Continuous Prediction," J. Neural Eng., vol. 20, no. 3, 2023.
- [17] V. V. Bauman and S. C. E. Brandon, "Gait Phase Detection in Walking and Stairs Using Machine Learning," *J. Biomech. Eng.*, vol. 144, no. 12, p. 121007, 2022.
- [18] Lie Yu, Pengzhi Mei, and Lei Ding, "Gait Pattern Recognition through Force Sensor Platform based on XGBoost Model and Harris' Hawks Optimization," *IAENG International Journal of Applied Mathematics*, vol. 55, no. 1, pp118-125, 2025.
- [19] Lie Yu, Gaotong Hu, Lei Ding, Na Luo, and Yong Zhang, "Gait Pattern Recognition based on Multi-sensors Information Fusion through PSO-SVM Model," *Engineering Letters*, vol. 32, no. 5, pp974-980, 2024.
- [20] M. Moodi, M. Ghazvini, and H. Moodi, "A Hybrid Intelligent Approach to Detect Android Botnet Using Smart Self-Adaptive

### **IAENG International Journal of Computer Science**

- Learning-Based PSO-SVM," Knowl.-Based Syst., vol. 222, p. 106988, 2021
- [21] Y. Cui et al., "Scale-Up Prediction of Supercritical CO2 Circulating Fluidized Bed Boiler Based on Adaptive PSO-SVM," *Powder Technol.*, vol. 419, p. 118328, 2023.
- [22] L. Kun, Y. Liu, S. Ji, C. Gao, S. Z. Zhang, and J. Fu, "A Novel Gait Phase Recognition Method Based on DPF-LSTM-CNN Using Wearable Inertial Sensors," *Sensors*, vol. 23, no. 13, pp5905, 2023.
- [23] F. L. Yu, J. B. Zheng, L. Yu, H. Xiao, Q. Chen and D. Zhang, "Transition Motion Pattern Classification for Lower Limb Exoskeleton in Stair Scenes based on CNN and GRU," *Journal of Mechanics in Medicine and Biology*, vol. 24, no. 10, pp2350085, 2024.